Immunity
Article

Spatiotemporal Regulation of T Cell Costimulation by TCR-CD28 Microclusters and Protein Kinase C θ Translocation

Tadashi Yokosuka,[1] Wakana Kobayashi,[1] Kumiko Sakata-Sogawa,[2] Masako Takamatsu,[1] Akiko Hashimoto-Tane,[1] Michael L. Dustin,[4] Makio Tokunaga,[3,5] and Takashi Saito[1,6,*]
[1]Laboratory for Cell Signaling
[2]Single Molecule Imaging
[3]Molecular Systems Immunology
RIKEN Research Center for Allergy and Immunology, 1-7-22 Suehiro-cho, Tsurumi-ku, Yokohama 230-0045, Japan
[4]Program in Molecular Pathogenesis, Skirball Institute of Biomolecular Medicine and Department of Pathology, New York University School of Medicine, 540 First Avenue, New York, NY 10016, USA
[5]Department of Biological Information, Graduate School of Bioscience and Biotechnology, Tokyo Institute of Technology, 4259 Nagatsuta, Midori-ku, Yokohama 226-8501, Japan
[6]WPI Immunology Frontier Research Center, Osaka University, 3-1 Yamadaoka Suita, Osaka 565-0871, Japan
*Correspondence: saito@rcai.riken.jp
DOI 10.1016/j.immuni.2008.08.011

SUMMARY

T cell activation is mediated by microclusters (MCs) containing T cell receptors (TCRs), kinases, and adaptors. Although TCR MCs translocate to form a central supramolecular activation cluster (cSMAC) of the immunological synapse at the interface of a T cell and an antigen-presenting cell, the role of MC translocation in T cell signaling remains unclear. Here, we found that the accumulation of MCs at cSMAC was important for T cell costimulation. Costimulatory receptor CD28 was initially recruited coordinately with TCR to MCs, and its signals were mediated through the assembly with the kinase PKCθ. The accumulation of MCs at the cSMAC was accompanied by the segregation of CD28 from the TCR, which resulted in the translocation of both CD28 and PKCθ to a spatially unique subregion of cSMAC. Thus, costimulation is mediated by the generation of a unique costimulatory compartment in the cSMAC via the dynamic regulation of MC translocation.

INTRODUCTION

T cells require two distinct signals for activation and differentiation: an antigen (Ag)-recognition signal transmitted through the T cell receptor (TCR) upon recognition of the Ag peptide-major histocompatibility complex (MHCp) on an antigen-presenting cell (APC), and a costimulatory signal transmitted through costimulatory receptors upon binding ligands expressed on APCs. Costimulatory signals are essential for the full activation of T cells for cytokine production, proliferation, survival, and functional differentiation. In order to induce proper activation of T cells through costimulation, expression of costimulatory receptors and their signals should be regulated in appropriate strength and timing in a dynamic and quantitative fashion. Modulation of costimulatory signals for T cell activation has been attempted in the clinical setting, including the modulation of autoimmune diseases, such as rheumatoid arthritis and psoriasis, prevention of graft versus host disease in transplantation, effective vaccinations, and augmented antitumor immunity (Riley and June, 2005; Salomon and Bluestone, 2001).

CD28, which is constitutively expressed on both naive and effector T cells, plays a predominant role in costimulation by binding its ligands, CD80 (B7-1) and CD86 (B7-2) (Acuto and Michel, 2003; Chambers et al., 2001; Rudd and Schneider, 2003; Sharpe and Freeman, 2002). CD86 is constitutively expressed at low amounts on most professional APCs and is rapidly upregulated after activation, whereas CD80 is inducibly expressed at a later time. Studies of genetically modified mice lacking CD28 or CD80/CD86 have confirmed that CD28 signals augment a variety of T cell functions, including cell-cycle progression, antiapoptotic function, cytokine production, T helper polarization, cytotoxic T cell differentiation, and humoral immunity maturation. In addition to these direct functions, CD28-mediated signals upregulate other costimulatory, cytokine, and chemokine receptors, consequently inducing secondary costimulatory responses. Although CD28 downstream signals have been extensively analyzed for more than a decade, the precise mechanisms are not clearly understood. Many molecules, such as phosphoinositide 3-kinase (PI3K) (Harada et al., 2003; Pages et al., 1994), lymphocyte-specific protein tyrosine kinase (Lck) (Holdorf et al., 1999; Liu et al., 2000), growth factor receptor-bound protein 2 (Grb2) (Raab et al., 1995), Grb2-related adaptor protein (Gads) (Watanabe et al., 2006), IL2-inducible T cell kinase (Itk), the guanine-nucleotide exchange factor Vav (Villalba et al., 2000), protein kinase B (PKB) (also known as Akt) (Kane et al., 2001), protein phosphatase 2A (PP2A) (Alegre et al., 2001; Chuang et al., 2000), and protein kinase C θ (PKCθ) (Villalba et al., 2000), have been implicated in CD28-mediated costimulatory signals. However, because these molecules also function in TCR downstream signals, it is difficult to parse CD28-specific cascades qualitatively and quantitatively.

Immune responses are initiated by the communication between Ag-specific T cells and APCs. An immunological synapse (IS) is formed at the T cell-APC interface and is made up of a central supramolecular activation cluster (cSMAC) containing the TCR-CD3 complex and a peripheral SMAC (pSMAC) containing the integrin LFA-1 (Grakoui et al., 1999; Monks et al., 1998). An IS is dynamically generated at the interface between a T cell and a B cell or a glass-supported planar bilayer, whereas there was a report describing a multifocal pattern of TCR, not cSMAC, between a T cell and a dendritic cell (DC) (Brossard et al., 2005). We have recently reported that T cell activation is spatiotemporally regulated by TCR microclusters (MCs) containing receptors, kinases, and adaptors (Bunnell et al., 2002; Campi et al., 2005; Saito and Yokosuka, 2006; Yokosuka et al., 2005). As the initial step of T cell activation, TCRs form small clusters at the interface between a T cell and an APC or a planar bilayer. Because these clusters contain both TCRs and phosphorylated proteins, and intracellular calcium concentrations are increased when a few MCs are generated, TCR MCs appear to function as signalsomes for T cell activation. As a subsequent step, only TCRs translocate to the center of the interface to result in cSMAC formation. TCR MCs containing kinases and adaptors are observed only at the peripheral edge of a T cell and not in cSMAC. These findings mainly from the planar bilayer system imply that TCR MCs are responsible for Ag recognition and the induction of activation signals both at initial contact and at a later stage for maintenance of activation, and that cSMACs are unable to sustain signaling (Varma et al., 2006). This concept of MCs serving as a key signalsome in T cell activation has raised important questions on how CD28-mediated costimulation is spatially and temporally regulated in the relationship with TCR MCs for the full activation of T cells.

CD28 was previously reported to traffic into the T cell-APC interface and to colocalize with PKCθ upon Ag recognition (Egen and Allison, 2002; Pentcheva-Hoang et al., 2004). Regarding the localization of CD28 in the IS, CD28 was reported to be localized at cSMAC (Bromley et al., 2001) or to be segregated from TCR in IS (Andres et al., 2004a; Huang et al., 2002; Tseng et al., 2005). Similar to TCR signals, CD28 signals were suggested to precede cSMAC formation because CD28 upregulated TCR-induced intracellular calcium within seconds after T cell-APC conjugation. It is also inferred that CD28 localized in lipid rafts and augments the recruitment of TCR downstream molecules to lipid rafts. However, the dynamic regulation of CD28 and its related signaling molecules is poorly understood.

We report here the results of molecular-imaging analysis of CD28-mediated costimulation. CD28 was recruited coordinately with TCR to MCs, and then PKCθ was recruited to TCR-CD28 MCs by association with CD28, thereby resulting in the initial activation of T cells. Furthermore, CD28 played a role in retaining PKCθ at a spatially unique and dynamic subregion of cSMAC, leading to sustained signals for T cell activation.

RESULTS

Cluster Formation of CD28 at TCR MCs and cSMACs

To examine the dynamic movement of CD28 on a live T cell, we visualized CD28 during T cell activation on a glass-supported planar bilayer by objective total internal reflection fluorescence microscopy (TIRFM) (Tokunaga et al., 1997). We performed retroviral infection to introduce EGFP-tagged CD28 (EGFP-CD28) into $CD4^+$ T cells from AND TCR-transgenic (AND-Tg) (specific for moth cytochrome *c* 88-103 [MCC88-103] on I-E^k) CD28-deficient (*Cd28*$^{-/-}$) mice. The T cells were allowed to settle onto a planar bilayer containing glycophosphatidylinositol (GPI)-anchored I-E^k loaded with MCC88-103, ICAM-1-, and CD80-GPI (I-E^k-ICAM-1-CD80) (Bromley et al., 2001; Grakoui et al., 1999), and EGFP-CD28 movement in the entire process of T cell-bilayer contact was imaged. The densities of I-E^k, ICAM-1, and CD80 were adjusted to equal those of lipopolysaccharide (LPS)-stimulated B cells, i.e., approximately 250, 100, and 60–120 molecules/μm^2, respectively (Figure 1A).

CD80/CD86 binding has been shown to enhance both T cell proliferation and IL-2 production as costimulatory functions. Because we previously demonstrated that CD80-GPI enhances IL-2 production by naive T cells on a planar bilayer (Bromley et al., 2001), we applied silica beads coated with the same I-E^k-ICAM-1-CD80-containing liposomes to stimulate T cells. AND-Tg naive T cells showed marked increases in IL-2 production, proliferation, and CD69 expression upon bead stimulation (Figures 1B–1D). Similar results were obtained with effector T cells (Figure S1, available online).

Similar to the clustering of TCR-CD3 (Campi et al., 2005; Yokosuka et al., 2005), CD28 was found to generate clusters at the T cell-bilayer interface as soon as a T cell attached, and the number of clusters increased during cell spreading. CD28 MC formation was completely dependent on the presence of CD80 (Figure 2A and Movies S1 and S2). After cSMAC formation, CD28 MCs continued to be generated at the periphery of the cell-bilayer interface and accumulated in the central region (Figure 2B and Movies S3 and S4). Then, we examined whether CD28 MCs move in a manner similar to TCR MCs, namely, colocalization initially with TCR MCs and later with cSMACs. Surprisingly, CD28 MCs colocalized with TCR MCs within the first few minutes of contact (Figure 2C). The average number of CD28 MCs is 136 ± 39.4 in ten representative cells at 2 min. Almost all of the CD28 MCs (93.9% ± 7.4%) initially overlapped with CD3. After cSMAC formation, a majority of CD28 translocated to the center but, unexpectedly, segregated from TCR; high-density regions of CD28 ($CD28^{hi}$) and CD3 ($CD3^{hi}$) segregated from each other, although the $CD28^{hi}$ region exhibited dim CD3 staining ($CD3^{dim}$) and the $CD3^{hi}$ region exhibited dim CD28 staining ($CD28^{dim}$) (Figures 2C and 2D). Compared to the cSMAC observed in the absence of CD28-CD80 interaction, $CD3^{hi}$ regions were less massive because $CD28^{hi}$ regions interfered with the formation of massive $CD3^{hi}$ regions. Collectively, $CD28^{hi}$ regions appeared to be localized at relatively outer regions of cSMACs. We also utilized a planar bilayer containing Cy5-labeled ICAM-1-GPI as a marker for pSMAC to investigate whether $CD28^{hi}$ regions localized in cSMAC or pSMAC. The ICAM-1 ring merged with LFA-1 and surrounded both $CD28^{hi}$ and $CD28^{dim}$ regions, indicating that these CD28 clusters are localized in a previously unexplored outer region of cSMAC (Figure 2E). Collectively, these data show that CD28 initially accumulates and localizes at TCR MCs upon Ag stimulation, and is later sorted to the outer region of cSMAC as a unique compartment in IS.

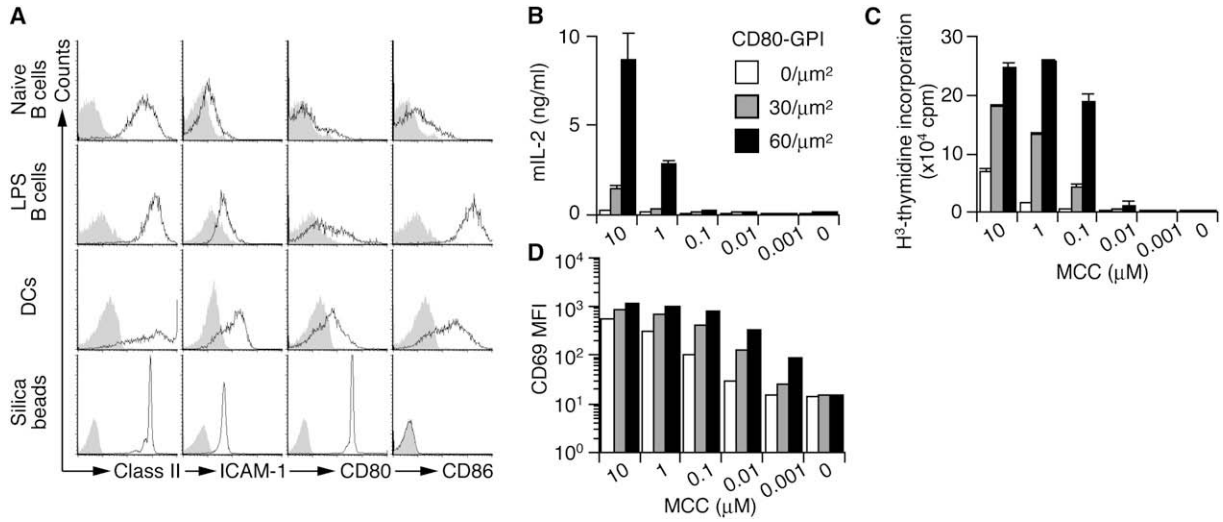

Figure 1. Costimulatory Function of CD80-GPI on Lipid Bilayers

(A) Five micron silica beads were coated with lipid bilayer containing I-E^k, ICAM-1, and CD80 at the same ratio as that for planar bilayers. Naive and LPS-stimulated B cells, DCs, and silica beads were stained with anti-class II, ICAM-1, CD80, or CD86 and analyzed by FACS.

(B–D) Naive $CD4^+$ T cells from AND-Tg mice were stimulated with silica beads that were coated with lipid bilayer containing I-E^k, ICAM-1, and CD80 at various densities and were prepulsed with indicated doses of MCC88-103. (B) IL-2 production was measured by ELISA at 48 hr, (C) proliferation was measured by ^{3}H-thymidine uptake at 60 hr, and (D) CD69 expression was measured by FACS at 6 hr after stimulation. Graphs (B and C) show mean ± standard deviation (SD) (n = 3). A representative of three independent experiments is shown.

Ligand-Dependent but Signal-Independent Formation of CD28 Clusters

To examine whether particular downstream signals of CD28 are required for MC formation, we reconstituted various EGFP-tagged wild-type (WT) or mutant CD28 into AND-Tg *Cd28*$^{-/-}$ T cells. Each EGFP-CD28 mutant contained a mutation in CD80/CD86 binding site (Y123A), dimerization (C142S), or PI3K, Grb2, and Gads binding site (Y189F), or a deletion of cytoplasmic 16 amino acids critical for lipid-raft association (Δ16) or the entire cytoplasmic tail (ΔCP) (Andres et al., 2004b; Holdorf et al., 1999; Pages et al., 1994; Schneider et al., 1995). The surface expression of all CD28 mutants was nearly equal on activated T cells (data not shown). We found no substantial differences in CD28 MC formation and distribution both at initial contact and after cSMAC formation among all CD28 mutants except Y123A. Y123A failed to form CD28 MCs, whereas even the CD28ΔCP mutant formed MCs (Figure 3), indicating that CD28 MC formation depends on CD28-CD80 binding but not on downstream signals of CD28. Nonetheless, the CD28 cytoplasmic domain may still recruit or associate with specific signaling molecules for costimulation.

CD28 Cluster and Its Downstream Signals

We analyzed a set of candidate molecules that move and colocalize with CD28 on a planar bilayer. TCR-proximal signals were first analyzed by staining for phosphorylated CD3ζ (Figure S2) or the kinase Zap70 (data not shown), but their phosphorylation status was not altered by the presence of CD80-GPI (Herndon et al., 2001). Then, we analyzed PI3K as a likely candidate for mediating costimulation because PI3K was clearly demonstrated to bind to the "YMNM" motif of CD28 cytoplasmic tail and to augment IL-2 production (Harada et al., 2003; Truitt et al., 1994). When AND-Tg T cells expressing EGFP-p55α as an indicator of type I PI3K were plated on an I-E^k-ICAM-1-CD80 planar bilayer, p55α clusters were transiently observed at the entire cell-bilayer interface. However, they disappeared soon after moving toward the center and did not accumulate at cSMAC, similar to Zap70 and the adaptor SLP-76 (Yokosuka et al., 2005) (Figure S3A and data not shown). The presence of CD80-GPI on the planar bilayer resulted in a slight but significant enhancement of area (0.050 ± 0.026 μm^2 with CD80-GPI; 0.037 ± 0.024 μm^2 without CD80-GPI, p value < 0.001 with Student's t test) and fluorescence intensity of EGFP-p55α clusters (0.282% ± 0.160% with CD80-GPI; 0.182% ± 0.109% without CD80-GPI, p < 0.001 with Student's t test) (Figure S4), confirming that PI3K is recruited to and enriched at TCR-CD28 MCs through CD28-CD80 binding during initial activation. However, these movements of PI3K clusters did not simply correlate with the accumulation of CD28 at cSMAC. Two-color analysis of AND-TCR T cell hybridomas expressing both ECFP-CD28 and EYFP-p85α confirmed this result—the initial colocalization of PI3K with TCR-CD28 MCs and the dissociation from CD28 in cSMAC later (Figure S3B). Catalytic subunit p110δ showed similar movement to p55α and p85α (data not shown). Furthermore, we analyzed cluster formation of Grb2, Gads, Vav1, and Itk in AND-Tg T cells expressing each EGFP fusion protein because these molecules have been suggested to functionally correlate with CD28 costimulation. However, we observed no accumulation at cSMACs regardless of the presence of CD80-GPI (data not shown).

CD28-Mediated Translocation of PKCθ to T Cell-APC Interface

We then analyzed PKCθ movement by using the assay described above, because PKCθ is activated after stimulation

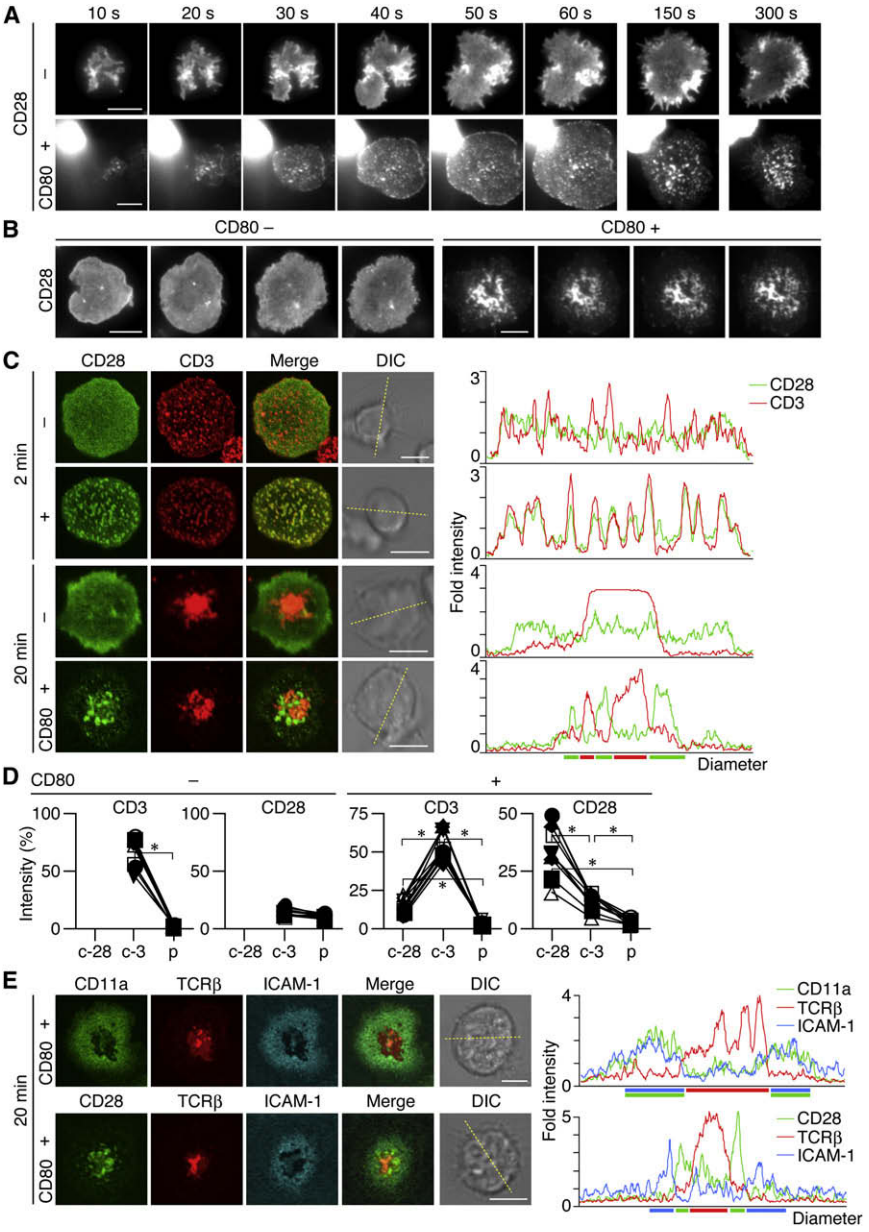

Figure 2. Ligand-Dependent Clustering of CD28 at TCR-CD3 MCs and at cSMAC

(A and B) AND-Tg T cells expressing EGFP-CD28 were plated on a planar bilayer containing (top) I-E^k and ICAM-1 plus (bottom) CD80 (prepulsed with MCC88-103). Cells were imaged at video rate (30 frames/s) with TIRFM (time shown above images). Images from 10 to 300 s are depicted in (A) and at 10 min after initial contact in (B). The interval between images is 10 s. Scale bars represent 5 μm. A representative of five independent experiments is shown. Real-time images in (A) and (B) are available in Movies S1–S4.

(C and D) Cells in (A) and (B) were fixed at 2 or 20 min after cell-bilayer contact, stained for CD3, and imaged by confocal microscopy. Histograms on right panels show fold fluorescence intensities of EGFP-CD28 (green) and CD3 (red) on the diagonal yellow lines in DIC images.

(D) Fluorescence intensities of CD3 and EGFP-CD28 in CD28 (c-28) or CD3 (c-3) clusters in cSMAC or pSMAC (p) were compared to the intensities of the entire interface in the cell in (C) bottom two rows (n = 10). *, p value < 0.001 with Student's t test. Scale bars represent 5 μm. A representative of three independent experiments is shown.

(E) AND-Tg T cells expressing EGFP-CD11a (top) or EGFP-CD28 (bottom) were stained with Alexa Fluor 546-labeled anti-TCRβ Fab and were plated on a planar bilayer containing I-E^k, CD80, and Cy5-labeled ICAM-1 (prepulsed with MCC88-103). Cells were imaged real time by confocal microscopy 20 min after contact. Histograms on the right panels are described as in (C). Scale bars represent 5 μm. A representative of two independent experiments is shown.

through both TCR and CD28 (Berg-Brown et al., 2004; Pfeifhofer et al., 2003; Sun et al., 2000), is segregated in IS with CD28 costimulation, is recruited to lipid raft, and plays a critical role in NF-κB activation. AND-Tg T cells expressing ECFP-CD28 and EYFP-PKCθ were conjugated with a dendritic cell line, DC-1, expressing I-E^k, ICAM-1, and transfected CD80, and the localization of CD28 and PKCθ was imaged. As previously reported (Huang et al., 2002), almost all T cells (96.6%, n = 56) showed clear accumulation and colocalization of CD28 with PKCθ as patched clusters on MCC88-103-pulsed CD80$^+$ DC-1 (Figures 4A–4C). Importantly, a majority of T cells (81.7%, n = 83) exhibiting conjugate formation with CD80$^-$ DC-1 showed PKCθ patch 2 min after conjugation, whereas only a minor population (1.6%, n = 62) showed the patch 20 min later (Figure 4C). These data suggest that Ag stimulation in the absence of CD80 induces transient translocation of PKCθ to the plasma membrane (Figure 4A, row 3; Figure 4B, top; and Figure 4C, left) and that the CD28-CD80 interaction is required for the coclustering of CD28 and PKCθ and for the stable and sustained translocation of PKCθ to the T cell-APC interface (Figure 4A, bottom; Figure 4B,bottom; and Figure 4C, right).

We further analyzed the kinetics and distribution of PKCθ by using a planar bilayer and AND-Tg T cells expressing EGFP-PKCθ. PKCθ clusters were transiently observed even in the absence of CD80-GPI (Figure 4D, top and Movie S5). In contrast, PKCθ accumulated to form clear clusters and persisted on the bilayer with CD80-GPI at initial activation (Figure 4D, bottom and Movie S6). Furthermore, after cSMAC formation, PKCθ clusters accumulated at the central region of the cell-bilayer interface in an annular form, which lasted for at least 60 min (Figure 4E and Movies S7 and S8). These data demonstrated that CD28-CD80 interaction enhanced the accumulation of PKCθ both at MCs initially and at the central region of cell-bilayer interface after cSMAC formation.

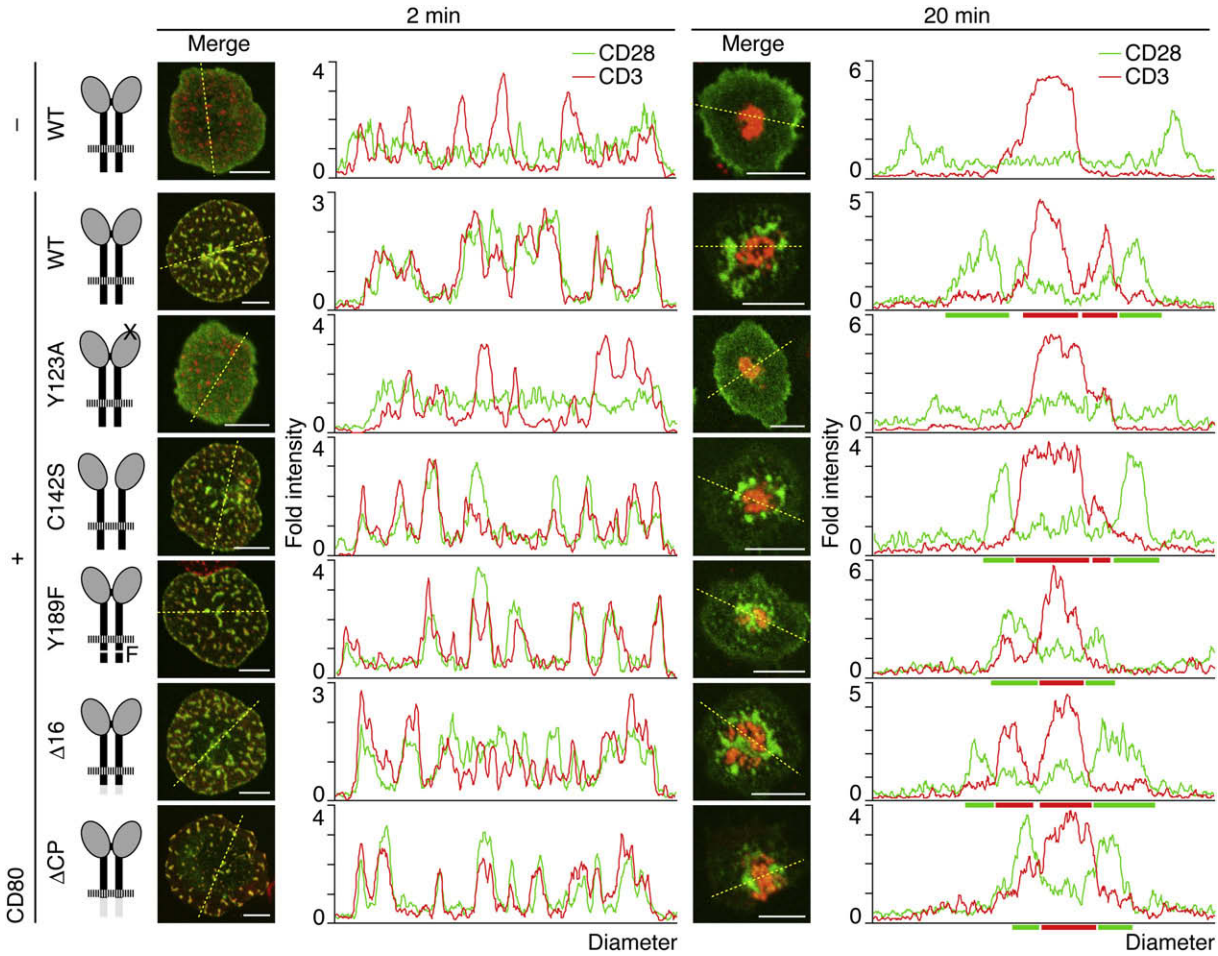

Figure 3. CD28 Cluster Formation Is Independent of CD28 Cytoplasmic Tail

AND-Tg T cells from *Cd28*$^{-/-}$ mice were reconstituted with EGFP-WT (top two rows) or mutant CD28 (bottom five rows, Y123A, C142S, Y189F, Δ16, and ΔCP) by retroviral infection. Cells were plated on a planar bilayer containing I-E^{k} and ICAM-1 (top row) plus CD80 (bottom six rows) (prepulsed with MCC88-103), fixed 2 min (left columns) or 20 min (right columns) after contact, and stained for CD3. The localizations of CD28 (green) and CD3 (red) were imaged by confocal microscopy, and the fold fluorescence intensities on diagonal yellow lines are shown by histograms. Scale bars represent 5 μm. A representative of three independent experiments is shown.

CD28-Mediated Localization of PKCθ at TCR MCs and cSMACs

Next, we examined whether PKCθ clusters colocalized with TCR or CD28 during initial and sustained activation. Costaining of PKCθ clusters with CD3 revealed that almost all PKCθ clusters (95.2%, n = 1302 in ten cells) merged with TCR MCs at initial contact (Figure 5A, top). After cSMAC formation, a majority of T cells (76.5%, n = 132) showed PKCθ accumulation in the CD3^{dim} region in an annular form and exclusion from the CD3^{hi} region in cSMACs (Figure 5A, bottom and Figure 5B). Because this PKCθ accumulation resembles that of CD28 clusters, we examined the colocalization of CD28 with PKCθ by using AND-Tg *Cd28*$^{-/-}$ T cells expressing both EYFP-PKCθ and ECFP-CD28 on a planar bilayer. Depending on CD28-CD80 interaction, almost all cells (93.4%, n = 61) initially exhibited colocalization of PKCθ with TCR-CD28 MCs (Figures 5C and 5D, and Figure S5A). Thereafter, PKCθ translocated to and accumulated at the center of the interface. After cSMAC formation, PKCθ persistently localized with CD28 at the outer region of cSMAC by segregating from core CD3 (Figures 5E and 5F, and Figure S5B). A majority of the cells with the annular form of CD28 clusters (81.8%, n = 33) colocalized with both PKCθ clusters and the CD3^{dim} region. As shown in Figure 2E, the annular form of PKCθ-CD28 clusters settled in cSMACs (Figure 5G). PKCθ and CD28 clusters in the annular form were also imaged at the interface between EGFP-PKCθ-expressing AND-Tg T cells and DC-1, although the frequency was lower and the images were less clear compared to those in the planar bilayer, probably as a result of membrane ruffling and variety expression of costimulatory receptor ligands on APCs (Figure S6 and Movie S9).

To understand the mechanism of CD28-mediated PKCθ recruitment, we examined the physical association between CD28 and PKCθ. Indeed, we found that PKCθ was coprecipitated with CD28 in lysates from T cell hybridomas expressing both ECFP-CD28 and EYFP-PKCθ (the same cells as those for imaging in Figures 4A and 4B) upon PMA stimulation (Figure 5H,

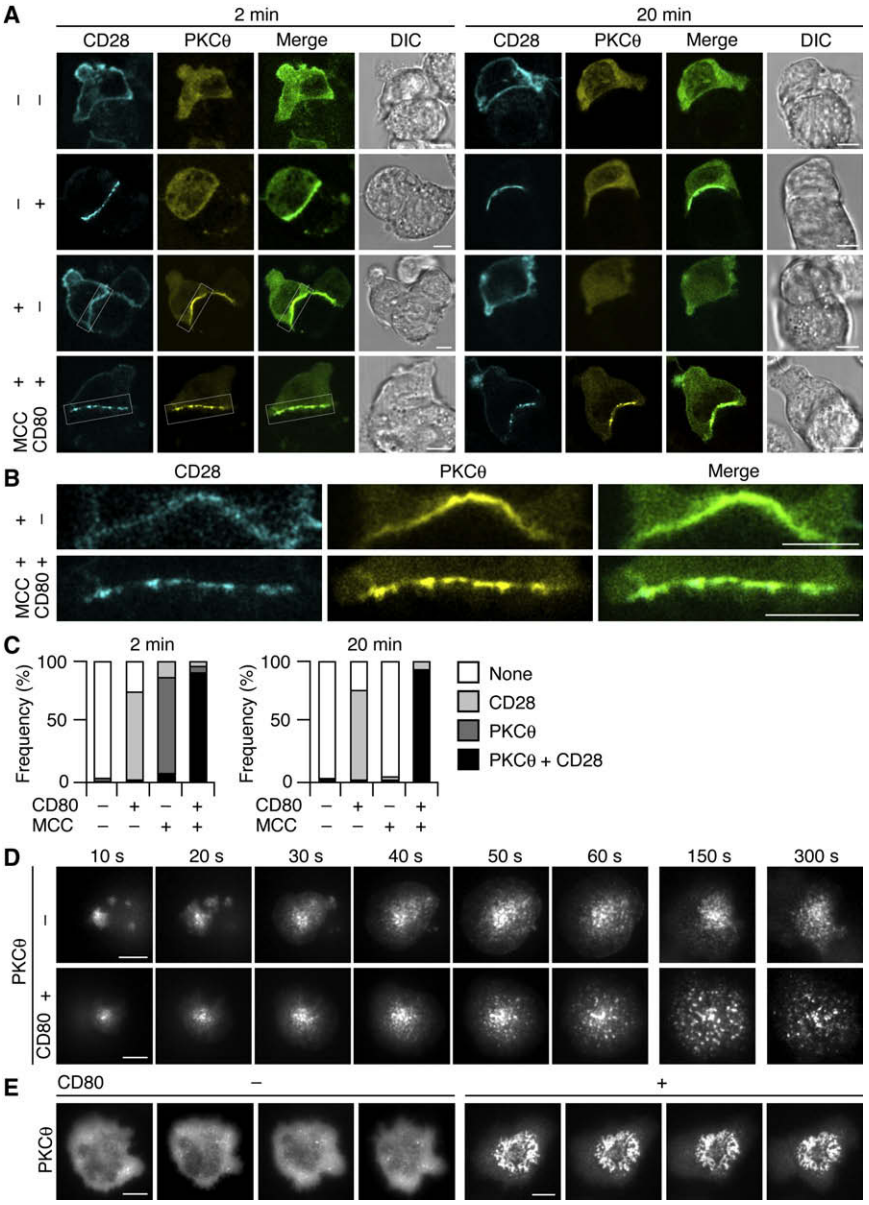

Figure 4. CD28-CD80 Binding Maintains PKCθ Translocation to Cell-Cell and Cell-Bilayer Interface

(A and B) AND-TCR T cell hybridomas expressing ECFP-CD28 and EYFP-PKCθ were conjugated with MCC88-103-pulsed or unpulsed DC-1, expressing or not expressing CD80, and imaged by confocal microcopy 2 min or 20 min after conjugation. Magnified images of the areas enclosed by white squares in (A) are depicted in (B). Scale bars represent 5 μm. A representative of three independent experiments is shown.

(C) Conjugated pairs in (A) were categorized by translocation of ECFP-CD28 and/or EYFP-PKCθ at the interface (2 min, n = 32, 108, 83, and 56; 20 min, n = 70, 63, 62, and 44, from left to right). A representative of three independent experiments is shown.

(D and E) AND-Tg T cells expressing EGFP-PKCθ were plated on a planar bilayer containing I-E^k and ICAM-1 (top) plus CD80 (bottom) (prepulsed with MCC88-103). Cells were imaged at video rate (30 frames/s) with TIRFM (time shown above images). Images from 10 to 300 s are depicted in (D) and at 10 min after initial contact, in (E), and the interval between images is 10 s. Scale bars represent 5 μm. A representative of five independent experiments is shown. Real-time images in (D) and (E) are available in Movies S5–S8.

left four columns in PMA [–] and [+]). More importantly, this physical association was identified in both effector and naive T cells from mice upon PMA stimulation (Figure 5I and data not shown). The CD28-PKCθ assembly appears to be weak because the association was detectable only with mild detergent, such as digitonin (Figure S7). These results suggest that CD28 recruits PKCθ by forming the assembly, although there is no evidence of the direct interaction of CD28 with PKCθ.

5C.C7-Tg T cells, whose Ag specificity is the same as that of AND-Tg T cells, generate smaller cSMACs because they have lower TCR affinity than AND-Tg T cells upon stimulation with the same concentrations of Ag on a planar bilayer. Under the condition in which cSMACs were not well formed by 5C.C7-Tg T cells with lower concentrations of MCC88-103 (1 and 0.1 μM), PKCθ still accumulated in an annular form (Figure S8). This result suggests that the annular accumulation of PKCθ clusters takes place without strong TCR-MHCp binding, which leads to clear cSMAC formation, but is dependent on CD28-CD80 binding.

Dynamic Maintenance of CD28-PKCθ Clusters at cSMAC

The critical role of CD28 in retaining PKCθ at cSMAC was confirmed by interrupting CD28-CD80 binding, via Ig fusion proteins of WT cytotoxic T lymphocyte antigen-4 (WT CTLA-4 Ig). The formation of both CD28 and PKCθ clusters in an annular form was diminished by the addition of WT CTLA-4 Ig but not Y139A (YA) CTLA-4, a binding mutant for CD80/CD86. The percentage of cells forming annular CD28 and PKCθ clusters was reduced from 87.2% to 32.4% and from 42.3% to zero, respectively (Figures 6A and 6B). Severe reduction of IL-2 production was observed when CD28-CD80 binding was blocked by WT CTLA-4 Ig at 2 min after stimulation, when only TCR-CD28-PKCθ-containing MCs were generated, as well as at 10 min after stimulation, when CD28-PKCθ annular clusters were set up (Figure 6C). Because most PKCθ molecules accumulated at CD28 clusters after cSMAC formation, these results suggest that both initial MCs and the annular form of PKCθ clusters are correlated with T cell function.

To further analyze CD28 function in the recruitment of PKCθ to the plasma membrane, we examined the relocalization of PKCθ at CD28 clusters. In our systems, CD28 MCs were generated, and these MCs accumulated at the central region of the interface

between T cells and I-E^k-ICAM-1-CD80 planar bilayers without MCC88-103. PKCθ was mainly localized in cytosol without Ag stimulation; however, it efficiently translocated to CD28 clusters upon PMA stimulation (Figures 6D and 6E). These results suggest that CD28 clusters recruit and retain PKCθ and induce the formation of the annular form of PKCθ clusters.

TCR clusters in cSMAC were found to be relatively stable on the basis of a fluorescence recovery after photobleaching (FRAP) study (Grakoui et al., 1999). We investigated the dynamics of annular forms of CD28 and PKCθ clusters in cSMAC by FRAP (Figures 6F and 6G and Movies S10 and S11). Indeed, both CD28 and PKCθ showed rapid recovery of their clusters, indicating active maintenance of the structure and dynamic exchange within cSMAC. PKCθ exhibited more rapid and complete recovery than CD28, probably as a result of its higher mobility as a cytoplasmic protein. These data suggest that the cytoplasmic tail of CD28 functions to dynamically recruit and concentrate PKCθ by specific association, and they indicate that the annular form of PKCθ clusters is dynamically generated and maintained by recruiting CD28-PKCθ from peripheral TCR-CD28 MCs.

Furthermore, PKCθ clusters in the annular form were stained with anti-phospho-PKCθ at the outer region of cSMAC in a CD28-CD80-dependent manner in normal T cells, although a question on the antibody specificity has been raised (Lee et al., 2005) (Figure S9). The result suggests that PKCθ that accumulated in the annular form was active in the induction of costimulatory signals.

Regulation of PKCθ Translocation to TCR-CD28 MCs by CD28 Signals

To examine the requirement of the cytoplasmic tail of CD28 for PKCθ translocation to TCR-CD28 MCs, we established a series of AND-TCR T cell hybridomas expressing EYFP-PKCθ and various ECFP-CD28 mutants. First, we analyzed the translocation of PKCθ to the T cell-APC interface by using DC-1 with or without CD80 expression (Figures 7A and 7B). WT CD28 exhibited colocalization with PKCθ at the T cell-APC interface upon Ag stimulation 2 min and 30 min after conjugation. As in Figure 4A, 2 min after T cell-APC conjugation, the translocation of PKCθ to the interface in T cells expressing CD28 with the mutated or deleted cytoplasmic tail (Y189F, Δ16, and ΔCP) was similar to that in T cells expressing WT CD28. In contrast, PKCθ patches that colocalized with CD28 showed a decrease in number in T cells expressing CD28 with the mutated or deleted cytoplasmic tail (Y189F, Δ16, and ΔCP) 30 min after conjugation (Figure 7B). The colocalization of CD28 with PKCθ was further analyzed on the planar bilayer with AND-Tg *Cd28*$^{-/-}$ T cells (Figure 7C) and AND-TCR T cell hybridomas (Figure 7D and Figure S10). Whereas CD28 MCs were generated independently of the cytoplasmic tail of CD28, PKCθ was not clearly recruited and did not form MCs if the cytoplasmic tail was mutated or deleted (Figure 7C and Figure S10). These data demonstrate that CD28 MC formation is independent of, but lasting recruitment of PKCθ to CD28 MCs is completely dependent on, the cytoplasmic tail of CD28. Quantification of the number of AND-TCR T cell hybridomas exhibiting colocalization of PKCθ clusters with WT or mutant CD28 clusters is shown in Figure 7D. Consistent with these imaging data, biochemical analysis revealed that the physical association between PKCθ- and CD28-bearing cytoplasmic tail mutations was much weaker than that between PKCθ and WT CD28 (Figure 5H). To clarify the function of the colocalization of CD28 with PKCθ within the same TCR MCs, we reconstituted AND-Tg T cells from *Cd28*$^{-/-}$ mice with these CD28 mutants and stimulated with anti-CD28 plus PMA to analyze costimulatory function (Figure 7E). We noted a strong correlation among CD28-PKCθ colocalization, physical association, and CD28-mediated costimulation, suggesting that CD28-mediated costimulation for the full activation of T cells is mediated by the recruitment of PKCθ to TCR-CD28 MCs.

DISCUSSION

In this study, we illustrated the dynamic aspects of CD28-mediated costimulation in relation to TCR MCs. CD28 colocalizes with TCR to form TCR-CD28 MCs together with signaling molecules as signalsomes, where CD28 plays a critical role in recruiting PKCθ to MCs at initial activation, and then to the outer region of cSMAC, possibly for sustained activation to exhibit effector functions. Previous studies have indicated that TCR MCs generated at the periphery of IS induce activation signals, whereas cSMAC may not be responsible for transducing activation signals, because phosphorylated proteins are detected almost in peripheral MCs and not in cSMAC (Yokosuka et al., 2005), and that Ca^{2+} signaling is not sustained in the absence of peripheral MCs (Varma et al., 2006). However, the present result of CD28-PKCθ signaling at the outer region of cSMAC leads to the idea that cSMAC also provides signal competency for costimulation and that different signal clusters are responsible for TCR-mediated and costimulatory signals for the maintenance of T cell activation.

The translocation of CD28 to the T cell-APC interface before cSMAC formation was previously reported (Andres et al., 2004a), but we demonstrated that CD28 colocalizes with TCR and its downstream molecules as a TCR-CD28 MC. This colocalization of TCR with CD28 in the same MC coincides with the findings that CD28 shares most of the downstream molecules with TCR. We searched for a molecule that contributes specifically to CD28 signals by colocalizing initially with TCR MCs and then translocating to CD28 clusters at the outer region of cSMAC. Although CD28 signal enhanced the colocalization of PI3K with CD28, PI3K clusters differ from that of CD28. Finally, we found that PKCθ met the criteria for the specific mediator of CD28 signals: accumulation at TCR-CD28 MCs initially and at cSMAC later.

PKCθ is known as a downstream molecule of CD28. PKCθ- and CD28-deficient animals revealed similar functional defects (Pfeifhofer et al., 2003; Sun et al., 2000), although the physical interaction has not been shown. We provided evidence of the functional assembly between CD28 and PKCθ in three aspects: (1) PKCθ is contained within early activation signalsomes as TCR-CD28 MCs and translocates to cSMAC with CD28; (2) the physical association of CD28 with activated PKCθ is demonstrated by coimmunoprecipitation; and (3) the early localization of PKCθ at MCs and the late at cSMAC are functionally associated with IL-2 production. The similar regulation was observed in B cells; CD19 enhanced B cell functions through its colocalization with B cell receptors (BCRs) and Syk as BCR MCs (Depoil et al., 2008).

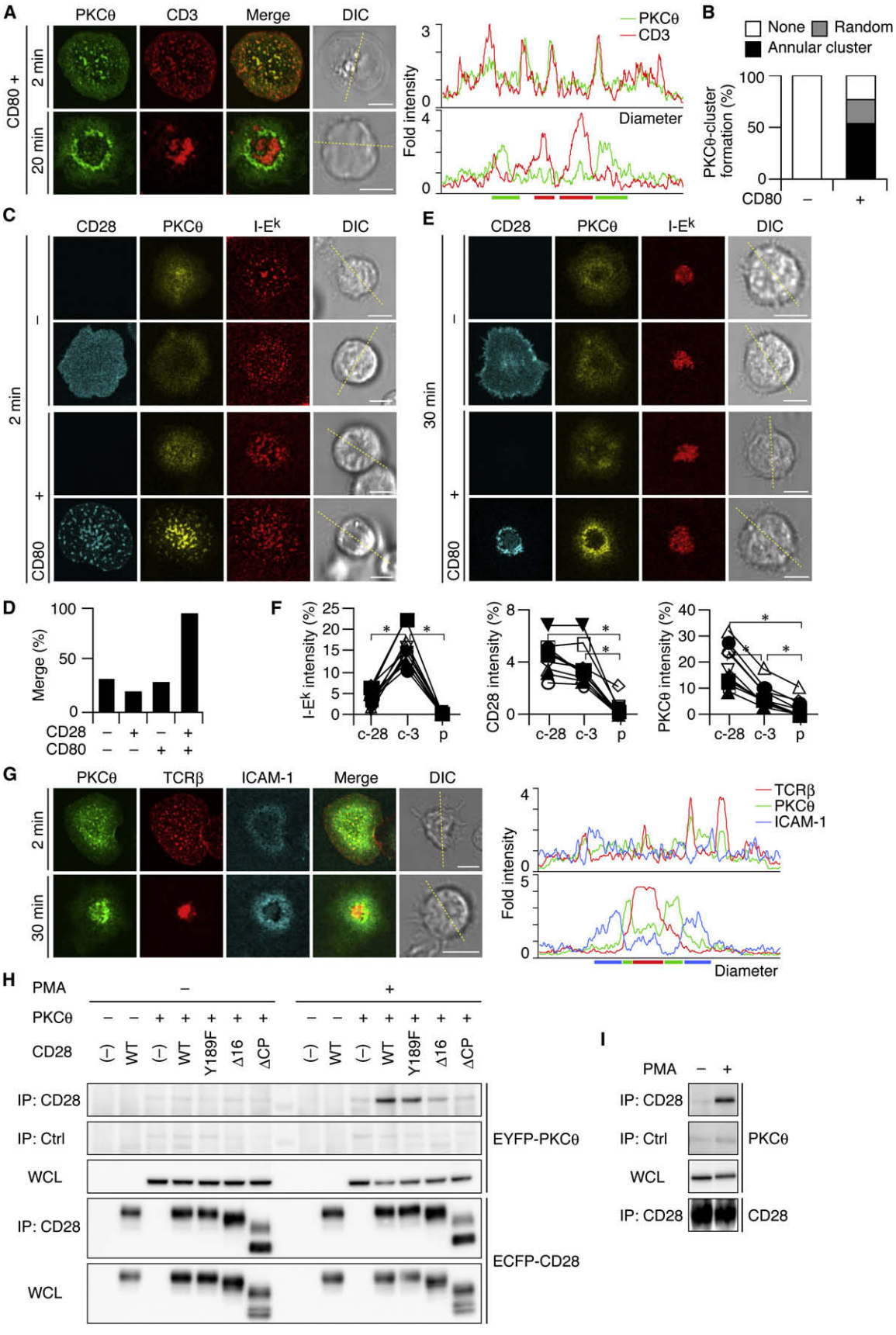
A
PKCθ
CD3
Merge
DIC
CD80 +
2 min
20 min
PKCθ
CD3
Fold intensity
Diameter
B
None
Random
Annular cluster
PKCθ-cluster formation (%)
CD80
C
CD28
PKCθ
I-Ek
DIC
2 min
CD80
D
Merge (%)
CD28
CD80
E
30 min
F
I-Ek intensity (%)
CD28 intensity (%)
PKCθ intensity (%)
c-28
c-3
p
G
TCRβ
ICAM-1
30 min
H
PMA
PKCθ
CD28
(–)
WT
Y189F
Δ16
ΔCP
IP: CD28
IP: Ctrl
WCL
EYFP-PKCθ
ECFP-CD28
I

PKCθ has been considered as a marker for cSMAC during T cell activation (Monks et al., 1998), whereas CD28 was suggested to play a role in segregation of PKCθ in IS (Huang et al., 2002; Tseng et al., 2005). In addition to the finding of colocalization of CD28-PKCθ in TCR MCs, we identified a unique functional subregion of cSMAC where CD28 and PKCθ accumulated. The generation of this subregion appears to depend on both localization and density of CD28 because PKCθ was colocalized in $CD28^{hi}$ but not TCR-$CD3^{hi}$ region. Furthermore, CD28 cluster formation depends on the density of CD28 and CD80/CD86 on T cells and APCs, and on the avidity of TCR, through the competition between CD28-CD80/CD86 and TCR-MHCp (unpublished data). We propose a functional region of cSMAC, $CD3^{dim}$ $CD28^{hi}$, as "costimulatory signalsome" for T cell activation. We demonstrated by FRAP analysis that no signal molecule translocated to the $CD3^{hi}$ region, and the $CD3^{dim}$ region was more flexible and dynamically regulated than the $CD3^{hi}$ region (unpublished data). The $CD3^{hi}$ region within cSMAC may be a negative regulatory compartment for T cell activation as suggested (Varma et al., 2006). The $CD3^{dim}$/$CD3^{hi}$ ratio appears to vary depending on the strength of TCR stimulation. A strong stimulus may induce more $CD3^{hi}$ region for endocytosis or degradation of TCR complexes, whereas a weak stimulus may result in more $CD3^{dim}$ regions that are susceptible to CD28-PKCθ-mediated costimulation. This is consistent with previous data suggesting negative regulatory functions of cSMAC by signal-strength-dependent TCR degradation (Cemerski et al., 2007). Our results suggest that cSMAC may inherit yin and yang functions for the regulation of T cell activation: endocytosis or degradation of the TCR complex for negative regulation through the $CD3^{hi}$ region, but CD28-PKCθ accumulation for sustained T cell signaling through the spatially distinct region.

Our data depicted both spatial and temporal differences in the dynamics of PKCθ and Zap70-SLP-76 for MC formation. PKCθ may be recruited to the plasma membrane via diacylglycerol (DAG) or in a phospholipase C-γ1 (PLCγ1)-DAG-independent manner (Villalba et al., 2002) and may be functionally activated by membrane translocation (Bi et al., 2001), whereas Zap70 and SLP-76 require phosphorylation for retention on the cell surface by associating with CD3 and LAT, respectively. Thus, PKCθ may associate with TCR-CD28 MCs via two steps—initial recruitment to the cell surface by DAG binding, followed by lateral movement to TCR-CD28 MCs through the association with CD28. The frequency of cells with PKCθ translocation in CD28 Y189F, PI3K-binding mutant was lower than that in Δ16 mutant, in both T cell-APC and T cell-bilayer experiments, whereas stimulation of Y189F CD28-expressing cells with PMA plus anti-CD28 augmented the proliferation, suggesting the involvement of PI3K in PKCθ membrane translocation and the partial rescue of T cell response by PMA-mediated PKCθ relocation.

CD28-mediated membrane translocation and the colocalization of CD28 with PKCθ could be explained by several mechanisms including recruitment into lipid raft and DAG-gradient. However, we failed to obtain the evidence to support these ideas (see Supplemental Data). Moreover, cell adhesion by CD28 may contribute to the functional recruitment of PKCθ to CD28 clusters through cytoskeletal rearrangement (Kaga et al., 1998). In this context, because filamin-A was reported to translocate into IS, associate with actin and PKCθ, and enhance IL-2 production in a CD28-CD80-dependent manner (Hayashi and Altman, 2006; Tavano et al., 2006), this mechanism might be involved in the colocalization of CD28 with PKCθ.

During T cell activation, the functional enhancement of T cell responses by CD28-mediated costimulation is prominent for T cell activation with weak TCR stimulus. Imaging studies have suggested that CD28 supports IL-2 production if no cSMAC is generated (Purtic et al., 2005) or if APC has a low concentration of Ag or self-Ag (Wulfing et al., 2002). In relation to these studies, we observed that CD28-PKCθ clusters could be generated even if cSMAC were not clearly generated with lower-affinity TCR, suggesting further differential regulation of two spatially distinct signaling clusters: Peripheral MCs and annular clusters in cSMAC may lead to different signaling pathways, such as Ca^{2+}-NFAT and NF-κB activation. The spatiotemporal regulation of TCR-CD28 MC formation in cSMAC may explain the complexity of intercommunicating molecules downstream of TCR and CD28.

Whereas CD28 localization in IS had been extensively investigated, nano-scale imaging of costimulatory receptor CD28 and its signal-transduction partners PI3K and PKCθ by TIRFM has

Figure 5. PKCθ Colocalizes with CD28 at TCR-CD3 MCs at Initiation and Forms Annular Clusters with CD28 after cSMAC Formation

(A and B) AND-Tg T cells expressing EGFP-PKCθ were plated on a planar bilayer containing I-E^k, ICAM-1, and CD80 (prepulsed with MCC88-103), fixed at the indicated times, and stained for CD3. Histograms show fold fluorescence intensities of PKCθ (green) and CD3 (red) on the diagonal yellow lines in DIC images. PKCθ clusters at 20 min (A, bottom) were categorized into random or annular clusters ([B], $CD80^-$, n = 85; $CD80^+$, n = 132). Scale bars represent 5 μm. A representative of two independent experiments is shown.

(C–F) AND-Tg T cells from *Cd28*$^{-/-}$ mice were transfected with EYFP-PKCθ (rows 1 and 3) plus ECFP-CD28 (rows 2 and 4) and plated on a planar bilayer containing Cy5-labeled I-E^k and ICAM-1 (top two rows) plus CD80 (bottom two rows). Cells were imaged by confocal microscopy 2 min (C) or 30 min after contact (E). Percentage of cells containing I-E^k clusters colocalizing with PKCθ clusters in (C) was calculated ([D], n = 30, 16, 34, and 61, from left to right). Colocalization of CD28, PKCθ, and I-E^k at cSMAC was analyzed (E), and fluorescence intensities of Cy5-I-E^k (left), ECFP-CD28 (middle), and EYFP-PKCθ (right) in CD28 (c-28) or CD3 (c-3) clusters in cSMAC or pSMAC (p) in (E) bottom row were compared to the intensities of entire cell-bilayer interfaces ([F], n = 10). *, p value < 0.001 with Student's t test. Scale bars represent 5 μm. A representative of three independent experiments is shown. Fold fluorescence intensities of ECFP-CD28, PKCθ, and I-E^k on the diagonal yellow lines in DIC images were depicted in histograms in Figure S5.

(G) AND-Tg T cells expressing EGFP-PKCθ were stained with Alexa Fluor 546-anti-TCRβ Fab and plated on a planar bilayer containing I-E^k, CD80, and Cy5-labeled ICAM-1. Cells were imaged by confocal microscopy 2 min (top) or 30 min after contact (bottom). Histograms are described as in (A). Scale bars represent 5 μm. A representative of two independent experiments is shown.

(H and I) Physical interaction between CD28 and PKCθ upon activation in T cell hybridomas (H) and normal splenic T cells (I). AND-TCR T cell hybridomas expressing EYFP-PKCθ and ECFP-WT or cytoplasmic mutant CD28 in Figure 3 were unstimulated (left) or stimulated for 2 min with 50 nM PMA (right). Cell lysates were immunoprecipitated with anti-CD28 (rows 1 and 4) or control (row 2) and blotted for EYFP-PKCθ (top three rows) and ECFP-CD28 (bottom two rows) (H). Splenic T cells were unstimulated (left) or stimulated (right) as in (H). Cell lysates were immunoprecipitated with anti-CD28 (rows 1 and 4) or control (row 2) and blotted with anti-PKCθ (top three rows) or anti-CD28 (bottom). WCL denotes whole-cell lysate. A representative of three independent experiments is shown.

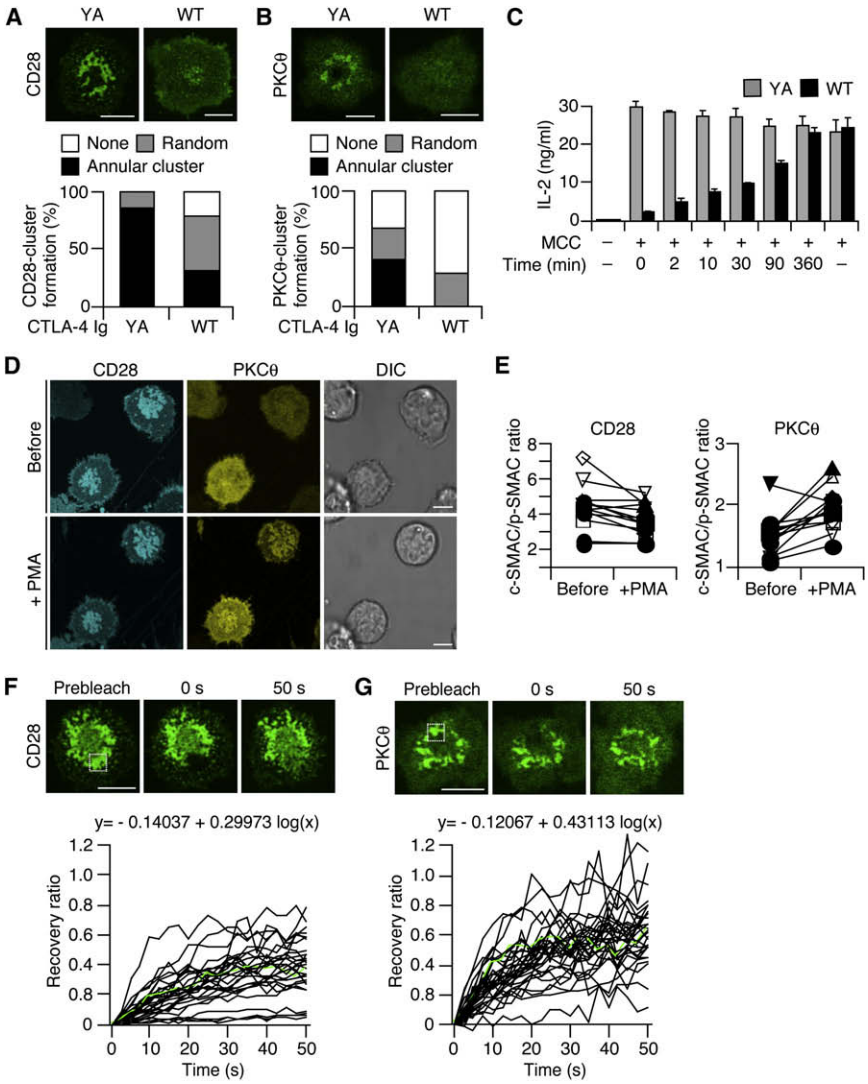

Figure 6. Dynamic Regulation of CD28-PKCθ Clusters in an Annular Form at cSMAC and Their Function in IL-2 Production

(A and B) 5C.C7-Tg T cells expressing EGFP-CD28 (A) or EGFP-PKCθ (B) were plated on a planar bilayer containing I-E^k, ICAM-1, and CD80 (prepulsed with MCC88-103) for 20 min and further incubated with WT or YA CTLA-4 Ig for 10 min. Cells were imaged by confocal microscopy and categorized into random or annular clusters (CD28 YA, n = 141; WT, n = 114; PKCθ YA, n = 52; WT, n = 44). Scale bars represent 5 μm. A representative of three independent experiments is shown.

(C) Reduction of IL-2 production by blocking CD28-CD80 interaction. 5C.C7-Tg effector T cells were stimulated by splenic B cells pulsed or unpulsed with MCC88-103, and WT (black) or YA CTLA-4 Ig (gray) was added at the indicated times. After 2 days, IL-2 was measured by ELISA. The graph shows mean ± SD (n = 3) obtained by two independent experiments.

(D and E) Relocalization of PKCθ to CD28 clusters. AND-TCR T cell hybridomas expressing both ECFP-CD28 and EYFP-PKCθ were plated on a planar bilayer containing I-E^k, ICAM-1, and CD80 without MCC88-103 and were allowed to develop CD28 clusters for 15 min. Translocation of EYFP-PKCθ in the same cells was imaged before and after 5 μM PMA stimulation (D). The average intensities of ECFP-CD28 (left) and EYFP-PKCθ (right) in cSMAC in the cells in (D) were compared to those of the entire interfaces ([E], n = 11). Scale bars represent 5 μm. A representative of two independent experiments is shown.

(F and G) Dynamism of CD28 and PKCθ clusters in an annular form. AND-Tg T cells expressing EGFP-CD28 (F) or EGFP-PKCθ (G) were plated on a planar bilayer as in (A) for 20 min. Recoveries of CD28 and PKCθ were analyzed by FRAP at specific regions (white square) of the annular clusters. Images were obtained every 2.5 s by confocal microscopy, and fluorescence recovery ratios were calculated ([F], n = 28; [G], n = 30). Green lines in graphs depict the recovery ratios of cells in top panels. Mathematical formulas are approximated curves involving 28 or 30 cells. Scale bars represent 5 μm. A representative of two independent experiments is shown. Real-time images in (F) (G) are available in Movies S9 and S10.

provided a new vision of the two costimulatory mechanisms that are functionally critical: the early recruitment of PKCθ and PI3K to TCR-CD28 MCs and the late formation of a dynamic subregion in cSMAC enriched with PKCθ but depleted of TCR and PI3K.

EXPERIMENTAL PROCEDURES

Reagents

Antibodies and reagents were purchased from the following suppliers: anti-mCD28, biotinylated anti-mCD3ε, FITC-anti-mCD11c, phycoerythrin (PE)-anti-mMHC class II, PE-mICMA-1, PE-anti-mCD69, PE-anti-mCD80, PE-anti-mCD86, and PE-isotype matched control Ig were from eBioscience; anti-PKCθ and anti-phospho PKCθ, from Santa Cruz; Alexa Fluor 647-anti-CD3 and Alexa Fluor 647-anti-phospho CD3ζ, from BD PharMingen; Alexa Fluor 488-streptoavidin, Alexa Fluor 647-anti-rabbit IgG, and Alexa Fluor 548-anti-hamster IgG, from Molecular Probes; and goat polyclonal anti-CD28 and rabbit polyclonal anti-PKCθ, from Santa Cruz. HRP-anti-GFP was from Miltenyi Biotec and phorbol 12-myristate 13-acetate (PMA) was from Sigma. Anti-mouse CD28 was provided by R. Abe (Science University of Tokyo, Japan).

Mice and Cells

AND-Tg and 5C.C7-Tg mice on *Rag2*$^{-/-}$ background were provided by R.N. Germain (National Institutes of Health, NIH) and K. Yasutomo (Tokushima University, Japan), respectively, and *Cd28*$^{-/-}$ mice were purchased from Jackson Laboratories. The DC line, DC-1, was provided by J. Kaye. T cell hybridoma expressing AND-TCR was established by cell fusion of activated AND-Tg CD4$^+$ T cells with TCR-negative BW5147, as previously shown (Kruisbeek, 1997).

Primary Cell Culture and Transduction

Expression constructs were transiently transduced into Phoenix packaging cells (provided by G. Norlan, Stanford University), via LipofectAmine Plus (Invitrogen). Retroviral supernatants were concentrated tenfold by centrifugation at 8000 × g for 12 hr. CD4$^+$ T cells were purified from AND-Tg *Rag2*$^{-/-}$ or AND-Tg *Cd28*$^{-/-}$ *Rag2*$^{-/-}$ mice and stimulated with 5 μM MCC88-103 (ANERADLIAYLKQATK) and irradiated spleen cells from B10.BR mice. One day after stimulation, the cells were suspended in the retroviral supernatant and

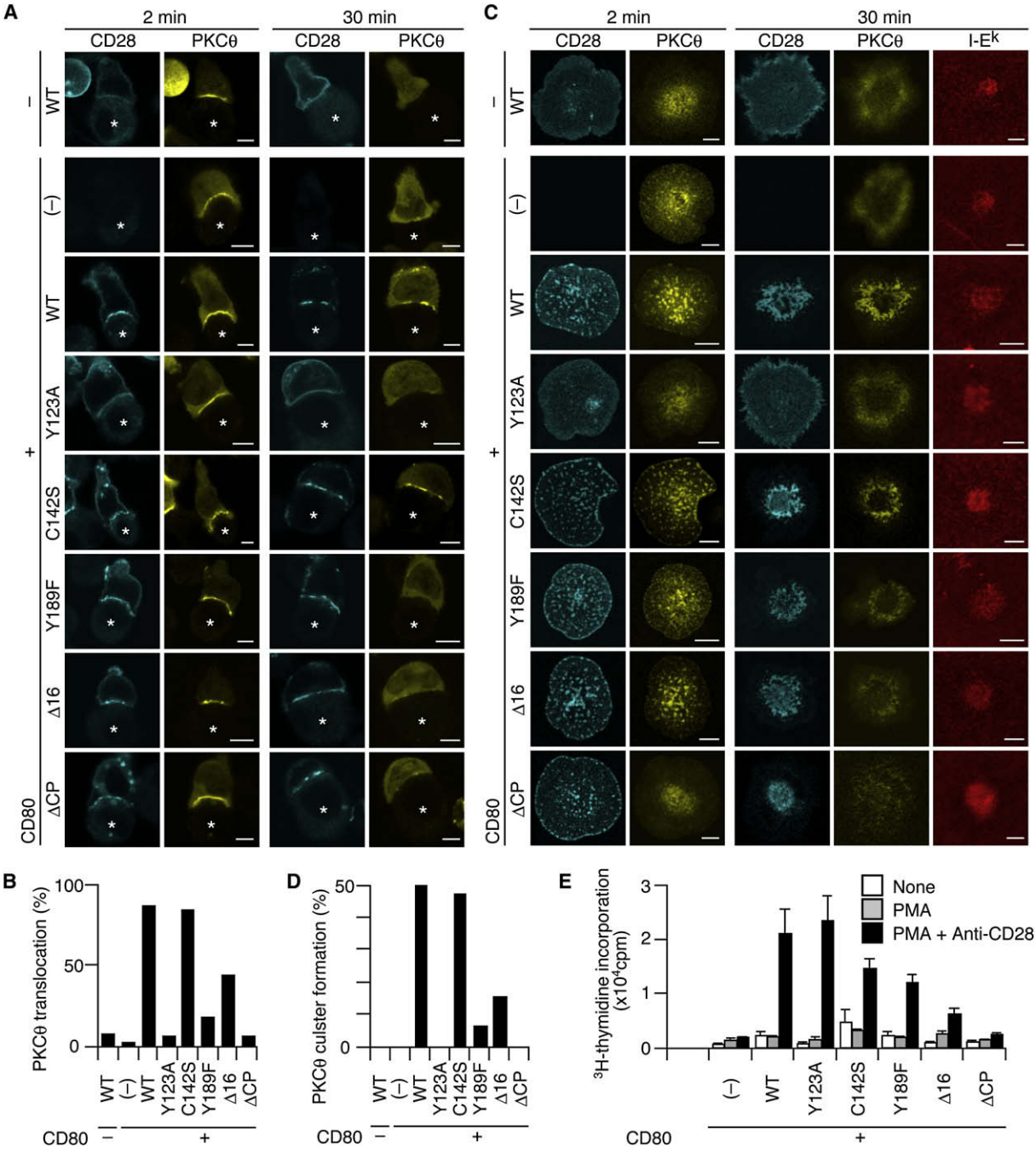

Figure 7. Function of CD28 Cytoplasmic Tail in the Translocation of PKCθ to T Cell-APC Interface and TCR-CD28 MCs

(A and B) AND-TCR T cell hybridomas expressing EYFP-PKCθ (yellow) and ECFP-WT or mutant CD28 (cyan) were conjugated with MCC88-103-pulsed DC-1 without ([A], top row) or with CD80 ([A], bottom seven rows). Cells were imaged real time at the indicated times by confocal microscopy. *, DC-1. Scale bars represent 5 μm. In fixed samples, conjugating pairs with PKCθ translocated to cell-cell interface were counted ([B], n = 60, 68, 60, 115, 68, 65, 73, and 122 from left to right). A representative of two independent experiments is shown.

(C) AND-Tg T cells from *Cd28*$^{-/-}$ mice were reconstituted with ECFP-WT or mutant CD28 (cyan) and EYFP-PKCθ (yellow), plated on a planar bilayer containing Cy5-I-E^{k} (red) and ICAM-1 plus CD80 (prepulsed with MCC88-103), and imaged by confocal microcopy in real time 2 min or 30 min after cell-bilayer contact. Scale bars represent 5 μm. A representative of four independent experiments is shown.

(D) AND-TCR T cell hybridomas in (A) were plated on a planar bilayer as in (C). Images were obtained in real time by confocal microscopy immediately after contact (Figure S10), and the percentages of cells containing PKCθ clusters are counted (n = 38, 26, 70, 42, 70, 83, 59, and 44 from left to right). A representative of two independent experiments is shown.

(E) AND-Tg T cells from *Cd28*$^{-/-}$ mice were reconstituted with WT or mutant CD28 and stimulated with PMA in combination with anti-CD28. T cell proliferation was measured 48 hr after stimulation. The graph shows mean ± SD (n = 3) obtained by three independent experiments.

centrifuged at 1000 × g for 90 min in the presence of 8 μg/ml polybrene (Sigma) and 200 U/ml human recombinant interleukin 2 (Ajinomoto). At day 3 or later, 20%–80% of T cells were transduced on the basis of EGFP, ECFP, or EYFP expression and sorted with FACSAria (BD) to obtain populations with homogenous fluorescence intensity. Cells were maintained for 5–14 days in RPMI1640 medium containing 10% FCS supplemented and recombinant IL-2.

Planar and Spherical Bilayers

GPI-anchored proteins of mouse I-E^k, ICAM-1, and CD80 were transfected into and purified from Chinese hamster ovary (CHO) or baby hamster kidney cells and were incorporated into dioleoyl phosphatidylcholine liposomes (DOPC, Avanti Polar Lipids). I-E^k- and ICAM-1-GPI were labeled with Cy5 mono NHS ester (Amersham Biosciences). Planar bilayers containing I-E^k-, ICAM-1-, and CD80-GPI were generated in a flow cell chamber system (Bioptechs). The expression levels of I-E^k, ICMA-1, and CD80 on the planar bilayer were quantified with 5-μm-diameter silica beads (Bangs Laboratories). Silica beads were loaded with DOPC containing I-E^k-, ICMA-1-, and CD80-GPI at the same concentrations as those of the planar bilayer, stained with FITC-labeled anti-I-E^k (14-4-4), ICMA-1 (YN1/1), or CD80 (16.10A1), and analyzed by FACSCalibur (BD). The densities of I-E^k, ICMA-1, and CD80 on the bilayer were calculated on the basis of standard FITC beads (Bangs Laboratories) and adjusted to approximately 250, 100, and 60–120 molecules/μm^2, respectively. Planar bilayers were loaded with 10 μM MCC88-103 in citrate buffer, pH 4.5, for 24 hr at 37°C, blocked with 5% nonfat dried milk in PBS for 1 hr at 37°C, and left to stand in the assay medium. All planar bilayer experiments were performed in HEPES-buffered saline containing 1% FCS, 2 mM $MgCl_2$, and 1 mM $CaCl_2$.

TIRF Imaging

Cells were imaged with TIRFM as previously described (Tokunaga et al., 1997). A solid-state laser (488 nm, 20 mW; Sapphire 488-20-OPS, Coherent) and an inverted microscope (IX-81, Olympus, Japan) were used. Images were captured with an electron-bombarded charge-coupled device camera (C-7190-23; Hamamatsu Photonics).

Fluorescence Imaging with Planar Bilayer

Cells transduced with various fluorescent-tagged proteins or stained by Fab antibodies were real-time imaged by TIRFM or confocal microscopy. For immunofluorescence staining, cells on a planar bilayer were fixed with 4% paraformaldehyde and stained with indicated Abs in 1% BSA PBS 0.3% saponin for 30 min at 25°C after blocking with 1% BSA PBS 0.3% saponin. All images were collected on a Leica DMIRES2 system, and data were analyzed with Leica confocal software.

T Cell-APC Conjugation Assay

DC-1 cells were prepulsed overnight at 37°C with 5 μM MCC peptide and washed before assay. AND-TCR T cell hybridomas (2.5×10^4) expressing ECFP-CD28 and/or EYFP-PKCθ were cultured with DC-1 on a glass-bottomed dish for real-time imaging, or on 12 mm coverslips for fixing and staining.

T Cell Stimulation with Silica Beads

$CD4^+$ T cells were prepared from AND-Tg mice on *Rag2*$^{-/-}$ background by magnetic cell sorting (Miltenyi Biotec). Naive or effector $CD4^+$ T cells ($5–10 \times 10^4$) were stimulated with silica beads coated with lipid bilayer containing I-E^k-, ICAM-1-, and CD80-GPI prepulsed with MCC88-103 in a 96-well round-bottomed dish. At 6 hr after stimulation, cells were stained with anti-CD69 and analyzed by FACSCalibur. At 48 hr, IL-2 in supernatants was measured by ELISA. Also at 48 hr, the cells were pulsed with 2 Ci/well of ^{3}H-thymidine for 12 hr, and the incorporated radioactivity was measured with a Microbeta scintillation counter (Amersham Pharmacia Biotech).

SUPPLEMENTAL DATA

Supplemental Data include Supplemental Experimental Procedures and ten figures and can be found with this article online at http://www.immunity.com/cgi/content/full/29/4/589/DC1/.

ACKNOWLEDGMENTS

We would like to thank R. Verma for discussion, J.P. Allison and R. Abe for reagents, R.N. Germain and K. Yasutomo for mice, and H. Yamaguchi and S. Kato for secretarial assistance. We especially thank the late T. Starr for instructions pertaining to planar bilayer preparation. This work was supported by a Grant-in-Aid for Priority Area Research from the Ministry of Education, Culture, Sports, Science, and Technology of Japan (T.Y., A.H.T., M.T., and T.S.), the New Energy Development Organization (M.T.), and the NIH (AI043542 and AI044931 to M.L.D.).

Received: April 21, 2008
Revised: July 5, 2008
Accepted: August 8, 2008
Published online: October 9, 2008

REFERENCES

Acuto, O., and Michel, F. (2003). CD28-mediated co-stimulation: A quantitative support for TCR signalling. Nat. Rev. Immunol. *3*, 939–951.

Alegre, M.L., Frauwirth, K.A., and Thompson, C.B. (2001). T-cell regulation by CD28 and CTLA-4. Nat. Rev. Immunol. *1*, 220–228.

Andres, P.G., Howland, K.C., Dresnek, D., Edmondson, S., Abbas, A.K., and Krummel, M.F. (2004a). CD28 signals in the immature immunological synapse. J. Immunol. *172*, 5880–5886.

Andres, P.G., Howland, K.C., Nirula, A., Kane, L.P., Barron, L., Dresnek, D., Sadra, A., Imboden, J., Weiss, A., and Abbas, A.K. (2004b). Distinct regions in the CD28 cytoplasmic domain are required for T helper type 2 differentiation. Nat. Immunol. *5*, 435–442.

Berg-Brown, N.N., Gronski, M.A., Jones, R.G., Elford, A.R., Deenick, E.K., Odermatt, B., Littman, D.R., and Ohashi, P.S. (2004). PKCtheta signals activation versus tolerance in vivo. J. Exp. Med. *199*, 743–752.

Bi, K., Tanaka, Y., Coudronniere, N., Sugie, K., Hong, S., van Stipdonk, M.J., and Altman, A. (2001). Antigen-induced translocation of PKC-theta to membrane rafts is required for T cell activation. Nat. Immunol. *2*, 556–563.

Bromley, S.K., Iaboni, A., Davis, S.J., Whitty, A., Green, J.M., Shaw, A.S., Weiss, A., and Dustin, M.L. (2001). The immunological synapse and CD28–CD80 interactions. Nat. Immunol. *2*, 1159–1166.

Brossard, C., Feuillet, V., Schmitt, A., Randriamampita, C., Romao, M., Raposo, G., and Trautmann, A. (2005). Multifocal structure of the T cell - dendritic cell synapse. Eur. J. Immunol. *35*, 1741–1753.

Bunnell, S.C., Hong, D.I., Kardon, J.R., Yamazaki, T., McGlade, C.J., Barr, V.A., and Samelson, L.E. (2002). T cell receptor ligation induces the formation of dynamically regulated signaling assemblies. J. Cell Biol. *158*, 1263–1275.

Campi, G., Varma, R., and Dustin, M.L. (2005). Actin and agonist MHC-peptide complex-dependent T cell receptor microclusters as scaffolds for signaling. J. Exp. Med. *202*, 1031–1036.

Cemerski, S., Das, J., Locasale, J., Arnold, P., Giurisato, E., Markiewicz, M.A., Fremont, D., Allen, P.M., Chakraborty, A.K., and Shaw, A.S. (2007). The stimulatory potency of T cell antigens is influenced by the formation of the immunological synapse. Immunity *26*, 345–355.

Chambers, C.A., Kuhns, M.S., Egen, J.G., and Allison, J.P. (2001). CTLA-4-mediated inhibition in regulation of T cell responses: Mechanisms and manipulation in tumor immunotherapy. Annu. Rev. Immunol. *19*, 565–594.

Chuang, E., Fisher, T.S., Morgan, R.W., Robbins, M.D., Duerr, J.M., Vander Heiden, M.G., Gardner, J.P., Hambor, J.E., Neveu, M.J., and Thompson, C.B. (2000). The CD28 and CTLA-4 receptors associate with the serine/threonine phosphatase PP2A. Immunity *13*, 313–322.

Depoil, D., Fleire, S., Treanor, B.L., Weber, M., Harwood, N.E., Marchbank, K.L., Tybulewicz, V.L., and Batista, F.D. (2008). CD19 is essential for B cell activation by promoting B cell receptor-antigen microcluster formation in response to membrane-bound ligand. Nat. Immunol. *9*, 63–72.

Egen, J.G., and Allison, J.P. (2002). Cytotoxic T lymphocyte antigen-4 accumulation in the immunological synapse is regulated by TCR signal strength. Immunity *16*, 23–35.

Grakoui, A., Bromley, S.K., Sumen, C., Davis, M.M., Shaw, A.S., Allen, P.M., and Dustin, M.L. (1999). The immunological synapse: A molecular machine controlling T cell activation. Science *285*, 221–227.

Harada, Y., Ohgai, D., Watanabe, R., Okano, K., Koiwai, O., Tanabe, K., Toma, H., Altman, A., and Abe, R. (2003). A single amino acid alteration in cytoplasmic domain determines IL-2 promoter activation by ligation of CD28 but not inducible costimulator (ICOS). J. Exp. Med. *197*, 257–262.

Hayashi, K., and Altman, A. (2006). Filamin A is required for T cell activation mediated by protein kinase C-theta. J. Immunol. *177*, 1721–1728.

Herndon, T.M., Shan, X.C., Tsokos, G.C., and Wange, R.L. (2001). ZAP-70 and SLP-76 regulate protein kinase C-theta and NF-kappa B activation in response to engagement of CD3 and CD28. J. Immunol. *166*, 5654–5664.

Holdorf, A.D., Green, J.M., Levin, S.D., Denny, M.F., Straus, D.B., Link, V., Changelian, P.S., Allen, P.M., and Shaw, A.S. (1999). Proline residues in CD28 and the Src homology (SH)3 domain of Lck are required for T cell costimulation. J. Exp. Med. *190*, 375–384.

Huang, J., Lo, P.F., Zal, T., Gascoigne, N.R., Smith, B.A., Levin, S.D., and Grey, H.M. (2002). CD28 plays a critical role in the segregation of PKC theta within the immunologic synapse. Proc. Natl. Acad. Sci. USA *99*, 9369–9373.

Kaga, S., Ragg, S., Rogers, K.A., and Ochi, A. (1998). Stimulation of CD28 with B7–2 promotes focal adhesion-like cell contacts where Rho family small G proteins accumulate in T cells. J. Immunol. *160*, 24–27.

Kane, L.P., Andres, P.G., Howland, K.C., Abbas, A.K., and Weiss, A. (2001). Akt provides the CD28 costimulatory signal for up-regulation of IL-2 and IFN-gamma but not TH2 cytokines. Nat. Immunol. *2*, 37–44.

Kruisbeek, A.M. (1997). Production of mouse T cell hybridomas. In Current Protocals in Immunology, J.E. Coligan, ed. (New York: Wiley and Sons), pp. 3.14.1–3.14.11.

Lee, K.Y., D'Acquisto, F., Hayden, M.S., Shim, J.H., and Ghosh, S. (2005). PDK1 nucleates T cell receptor-induced signaling complex for NF-kappaB activation. Science *308*, 114–118.

Liu, Y., Witte, S., Liu, Y.C., Doyle, M., Elly, C., and Altman, A. (2000). Regulation of protein kinase Ctheta function during T cell activation by Lck-mediated tyrosine phosphorylation. J. Biol. Chem. *275*, 3603–3609.

Monks, C.R., Freiberg, B.A., Kupfer, H., Sciaky, N., and Kupfer, A. (1998). Three-dimensional segregation of supramolecular activation clusters in T cells. Nature *395*, 82–86.

Pages, F., Ragueneau, M., Rottapel, R., Truneh, A., Nunes, J., Imbert, J., and Olive, D. (1994). Binding of phosphatidylinositol-3-OH kinase to CD28 is required for T-cell signalling. Nature *369*, 327–329.

Pentcheva-Hoang, T., Egen, J.G., Wojnoonski, K., and Allison, J.P. (2004). B7–1 and B7–2 selectively recruit CTLA-4 and CD28 to the immunological synapse. Immunity *21*, 401–413.

Pfeifhofer, C., Kofler, K., Gruber, T., Tabrizi, N.G., Lutz, C., Maly, K., Leitges, M., and Baier, G. (2003). Protein kinase C theta affects Ca2+ mobilization and NFAT cell activation in primary mouse T cells. J. Exp. Med. *197*, 1525–1535.

Purtic, B., Pitcher, L.A., van Oers, N.S., and Wulfing, C. (2005). T cell receptor (TCR) clustering in the immunological synapse integrates TCR and costimulatory signaling in selected T cells. Proc. Natl. Acad. Sci. USA *102*, 2904–2909.

Raab, M., Cai, Y.C., Bunnell, S.C., Heyeck, S.D., Berg, L.J., and Rudd, C.E. (1995). p56Lck and p59Fyn regulate CD28 binding to phosphatidylinositol 3-kinase, growth factor receptor-bound protein GRB-2, and T cell-specific protein-tyrosine kinase ITK: Implications for T-cell costimulation. Proc. Natl. Acad. Sci. USA *92*, 8891–8895.

Riley, J.L., and June, C.H. (2005). The CD28 family: A T-cell rheostat for therapeutic control of T-cell activation. Blood *105*, 13–21.

Rudd, C.E., and Schneider, H. (2003). Unifying concepts in CD28, ICOS and CTLA4 co-receptor signalling. Nat. Rev. Immunol. *3*, 544–556.

Saito, T., and Yokosuka, T. (2006). Immunological synapse and microclusters: The site for recognition and activation of T cells. Curr. Opin. Immunol. *18*, 305–313.

Salomon, B., and Bluestone, J.A. (2001). Complexities of CD28/B7: CTLA-4 costimulatory pathways in autoimmunity and transplantation. Annu. Rev. Immunol. *19*, 225–252.

Schneider, H., Cai, Y.C., Prasad, K.V., Shoelson, S.E., and Rudd, C.E. (1995). T cell antigen CD28 binds to the GRB-2/SOS complex, regulators of p21ras. Eur. J. Immunol. *25*, 1044–1050.

Sharpe, A.H., and Freeman, G.J. (2002). The B7–CD28 superfamily. Nat. Rev. Immunol. *2*, 116–126.

Sun, Z., Arendt, C.W., Ellmeier, W., Schaeffer, E.M., Sunshine, M.J., Gandhi, L., Annes, J., Petrzilka, D., Kupfer, A., Schwartzberg, P.L., and Littman, D.R. (2000). PKC-theta is required for TCR-induced NF-kappaB activation in mature but not immature T lymphocytes. Nature *404*, 402–407.

Tavano, R., Contento, R.L., Baranda, S.J., Soligo, M., Tuosto, L., Manes, S., and Viola, A. (2006). CD28 interaction with filamin-A controls lipid raft accumulation at the T-cell immunological synapse. Nat. Cell Biol. *8*, 1270–1276.

Tokunaga, M., Kitamura, K., Saito, K., Iwane, A.H., and Yanagida, T. (1997). Single molecule imaging of fluorophores and enzymatic reactions achieved by objective-type total internal reflection fluorescence microscopy. Biochem. Biophys. Res. Commun. *235*, 47–53.

Truitt, K.E., Hicks, C.M., and Imboden, J.B. (1994). Stimulation of CD28 triggers an association between CD28 and phosphatidylinositol 3-kinase in Jurkat T cells. J. Exp. Med. *179*, 1071–1076.

Tseng, S.Y., Liu, M., and Dustin, M.L. (2005). CD80 cytoplasmic domain controls localization of CD28, CTLA-4, and protein kinase Ctheta in the immunological synapse. J. Immunol. *175*, 7829–7836.

Varma, R., Campi, G., Yokosuka, T., Saito, T., and Dustin, M.L. (2006). T cell receptor-proximal signals are sustained in peripheral microclusters and terminated in the central supramolecular activation cluster. Immunity *25*, 117–127.

Villalba, M., Coudronniere, N., Deckert, M., Teixeiro, E., Mas, P., and Altman, A. (2000). A novel functional interaction between Vav and PKCtheta is required for TCR-induced T cell activation. Immunity *12*, 151–160.

Villalba, M., Bi, K., Hu, J., Altman, Y., Bushway, P., Reits, E., Neefjes, J., Baier, G., Abraham, R.T., and Altman, A. (2002). Translocation of PKC[theta] in T cells is mediated by a nonconventional, PI3-K- and Vav-dependent pathway, but does not absolutely require phospholipase C. J. Cell Biol. *157*, 253–263.

Watanabe, R., Harada, Y., Takeda, K., Takahashi, J., Ohnuki, K., Ogawa, S., Ohgai, D., Kaibara, N., Koiwai, O., Tanabe, K., et al. (2006). Grb2 and Gads exhibit different interactions with CD28 and play distinct roles in CD28-mediated costimulation. J. Immunol. *177*, 1085–1091.

Wulfing, C., Sumen, C., Sjaastad, M.D., Wu, L.C., Dustin, M.L., and Davis, M.M. (2002). Costimulation and endogenous MHC ligands contribute to T cell recognition. Nat. Immunol. *3*, 42–47.

Yokosuka, T., Sakata-Sogawa, K., Kobayashi, W., Hiroshima, M., Hashimoto-Tane, A., Tokunaga, M., Dustin, M.L., and Saito, T. (2005). Newly generated T cell receptor microclusters initiate and sustain T cell activation by recruitment of Zap70 and SLP-76. Nat. Immunol. *6*, 1253–1262.